Journal of Robotics and Control (JRC)
Volume 4, Issue 2, March 2023
ISSN: 2715-5072, DOI: 10.18196/jrc.v4i2.17165

Development of a Virtual Environment-Based Electrooculogram Control System for Safe Electric Wheelchair Mobility for Individuals with Severe Physical Disabilities

Jane Phoebe Achieng Ogenga [1*], Waweru Njeri [2], Joseph Muguro [3]
[1, 2, 3] Center for Robotics and Biomedical Engineering, Department of Electrical & Electronic Engineering, Dedan Kimathi University of Technology, Kenya
Email: [1] phoebeachiengaj@gmail.com, [2] waweru.njeri@dkut.ac.ke [3] joseph.muguro@dkut.ac.ke
*Corresponding Author

Abstract*—Conventional wheelchairs are predominantly manual or joystick-operated electric wheelchairs. However, operating these wheelchairs can be difficult or impossible for individuals with severe physical disabilities. Due to losing control of their physical limbs, they depend on an attendant for assistance. As a remedy, bio-signals may be used as a control mechanism since they are readily available and can be acquired from any body part. This research proposes to use EOG signals to vail a control mechanism and test it in a virtual and actual electric wheelchair. The main contribution of the study is an investigation of the use of EOG to control an electric wheelchair in a virtual environment to determine safe control parameters for wheelchair use in complex environments. A customized data acquisition circuit was developed to acquire single-channel EOG signals using wet electrodes. The acquired signal was filtered and processed using feature extraction and classification techniques in MATLAB software. Two customized control environments were developed in Unity 3D, one with equally partitioned sections and the other with sections decreasing in size as the robot wheelchair approaches the target. Twenty-two test subjects (mean age 24.5, std 1.5) participated in the study, controlling the robot wheelchair in real-time with non or least instances of collision and oversteering. The system achieved an accuracy of 96.5% with a response time of 0.7s, translating to an ITR of 70.6 bits/min. Overall, the participants managed to navigate the virtual environment with a completion time of 101.94s ± 19.71 and 109.07s ± 13.25 for the male and female participants, respectively. In the scene with decreasing section sizes, 72% and 54% instances of collision and oversteering were reported, respectively, highlighting the need to consider the complexity of the control environment and the sufficiency of the participants' control skills to ensure safety in operations. The results confirm the usefulness of EOG as a control interface, with little or no need for recalibration. It provides a promising avenue for individuals with severe physical disabilities to operate wheelchairs independently in complex environments, enhancing their quality of life.

Keywords— Electrooculogram; Wheelchair; Classification; Virtual Environment; Safety; Control

I. INTRODUCTION

Physical disability may be due to birth disorders, old age, spinal cord damage, cerebral palsy, amyotrophic lateral sclerosis (ALS), and brain stem stroke, among other diseases that cause muscle impairment or affect neural pathways [1]. According to a World Health Organization (WHO) report, approximately 75 million people require wheelchairs [2]. This accounts for about 1% of the entire world population. However, a more significant percentage cannot access an appropriate and high-quality wheelchair [3]–[5].

Besides the problem of access to wheelchairs, these individuals are also faced with issues related to control mechanisms. The conventional wheelchair is designed to be operated using joysticks or be externally propelled by an attendant [6]–[9]. In the case of terminally disabled individuals, who have lost partial or complete control of their physical limbs, the use of joystick-operated wheelchairs is very challenging. To counter this challenge, researchers are adopting alternative control mechanisms to allow for the usability and inclusivity of people with disability (PWD). Amongst the approaches include voice-operated wheelchair control [10]–[12], bio-signals control, and gaze controls, amongst others [1], [4], [5].

As opposed to the other alternatives, the use of bio-signals has been on the rise in the control of wheelchairs. The reason for this is due to their availability and ease of acquisition. Some of the bio-signals that are typically used as an interface between machines and humans include the Electrooculogram (EOG) [13]–[16] Electroencephalogram (EEG) [5], [17]–[19] and the electromyogram (EMG) signal [18], [20]–[24]. Electrooculography (EOG) is a method of measuring the eyes' resting potential. The positive cornea and negative retina form an electric dipole that moves with the movement of the eyeball to generate the resting potential, producing positive and negative electric potential, respectively. The frequency range is 0.05Hz-50Hz, and the corneal retinal voltage range of the EOG signal is 50-3500uV. EOG can be acquired using single channels (horizontal or vertical eye movements) or multichannel (both horizontal and vertical eye movements) [1], [25]–[27].

EOG signals have been used in a variety of scientific fields. In [28], EOG was used to develop an EOG-based switch for a wheelchair for on/off control. Intentional blinks were discriminated against using a waveform detection algorithm and were used to issue on/off commands. The commands were issued when a blink corresponded to a

button's flash on the Graphical user interface (GUI). EOG can be used in home automation by issuing control commands through a microcontroller, thus controlling the cursor and other home appliances. This has been achieved by [28]–[30], where different devices, such as lights, fans, etc., were switched on/off when the eye was moved in the right, left, upward, or downward direction. EOG signals have also been used for mouse control, thus aiding patients with computer use [15], [31], [32]. The participants used eye movement in different directions to perform and select an operation, while they used intentional blinking to navigate the application. The authors of [1] and [20] combined EOG and EMG to control a robot arm. The EOG signal was used to control the robot arm joint movements. In contrast, the EMG signal was used for arm gripper control, thus facilitating the robot's grasp and release capability on the targeted object. The EOG was acquired using multichannel and discrimination based on the polarity of the first and second peaks of the signals. At the same time, EMG was distinguished from EOG in the vertical channel through its high amplitude.

In [33], a prosthetic arm was controlled using a PIC microcontroller that received commands from the EOG signal. Threshold values for the left-right eye movement and blinks were set in the microcontroller and used as the control signals for the robot arm activation.

Saakshi and Manoj [34] developed an EOG-based Human-Machine Interface (HMI) to control the 3R robot. The processed EOG signal was fed to a microcontroller to generate control commands transmitted to the receiver using an RF transmitter. The command combinations controlled the servo motors, allowing the robot arm to be directed accordingly (left, right, up, and down), achieving an accuracy of 90% on its movement.

In rehabilitation, EOG has been studied and applied to control the wheelchair [35]–[39]. For instance, Choudhari *et al.* [14] used only voluntary eye blinks (single, double, and triple) to generate control commands for wheelchair navigation. They used the number of peaks and multi-threshold approaches to distinguish the different blink types by setting the amplitude, duration, and speed threshold. An API was developed that transferred the command to the motor driver. In [40], an EOG and accelerometer signals were combined to control a wheelchair. The accelerometer was hand-controlled, and the generated signal was processed simultaneously with the generated EOG signals. The command signals were fed to the microcontroller attached to the motor driver, thus controlling the wheelchair direction.

Rajesh *et al.* [41] proposed a novel EOG-based HMI that offered 13 control commands. Different flash buttons represented the various commands on the GUI. The corresponding control commands were sent when the subject blinked in time with the button flash to choose the desired button. Other than the threshold mechanism that has been used in some studies to distinguish different eye movements [34]–[38], [40], [41], machine learning and deep learning algorithms have also been embraced for the same [42]–[45]. Machine learning has different algorithms that are used for classification. The main classifier algorithms include support vector machine (SVM) [45]–[47], linear discriminant analysis (LDA) [47], [48], K-nearest neighbors (KNN) [44], [45], [49], [50] random forest [48], [51] and Ensemble Classifier (EC) [45], [51], [52].

To control wheelchair direction using eye movement, a flexible hydrogel biosensor and Wavelet Transform Support Vector Machine (WT-SVM) algorithm were used [53]. The proposed flexible hydrogel biosensors collected EOG and strain-induced signals when placed on the forehead. An accuracy of 96% was achieved using the designed sensor after classification. In their comparison of artificial neural networks (ANN) and support vector machines (SVM) for the classification of EOG, Qi *et al.* achieved the highest accuracy by using an SVM classifier compared to ANN using ten statistical parameters [54]. Such accuracy levels were attributed to SVM's ability to generalize while having a low training time.

Learning to operate a wheelchair can be challenging for new wheelchair users since it requires acquiring some skills. The challenges include navigating confined spaces, passing through doors, dodging stationary and moving objects, and navigating uneven or slippery surfaces. When instructing new users in a clinical setting, it can be challenging to replicate such circumstances, and where possible, their training in an actual wheelchair might be unsafe. Additionally, it might be difficult to set aside enough time for wheelchair training to allow new users to learn all the abilities necessary to operate a wheelchair securely [55]–[58].

Virtual environment (VE)-based training, on the other hand, can enhance navigating skills while guaranteeing user safety and significantly lowering the chance of injuries. Additionally, through VE, learning can be maximized by manipulating environmental features during training. A study by Bigras *et al.* [59] indicates that the skills learned in virtual environment control are transferred to actual wheelchair driving.

Djeha *et al.* [60] combined EEG and EOG signals to control a wheelchair in a virtual environment. EEG was used to capture the vertical eye movement, while through EOG, horizontal eye movement was captured. The control was successful, with an accuracy of 93%.

A user's safety can also be compromised by misclassification by the system. Misclassification occurs when a classifier assigns a data point to another class/category than the one it should be assigned to [61]. For instance, in EOG, a classifier may classify a left-eye movement as a right-eye movement. This might jeopardize the user's safety and those around them, especially when the wheelchair is near obstacles. Another factor that may threaten the safety of a wheelchair user is the issuance of wrong commands. In this case, the user might issue a wrong command unintentionally in cases like lost focus [49].

Few researchers have focused on mitigating the effect of misclassification on control. From the literature review, authors in [62] focused on the issue by integrating a reinforcement learning (RL) algorithm in a virtual wheelchair control. The shared controller helped check the distance from

the wall, and in instances of misclassification, it redirects the wheelchair to a safe position.

From the challenges mentioned above, the wheelchair controller should be tested critically for robustness against various scenarios touching on persons with severe disabilities/illnesses. A fail-safe mechanism should be introduced that negates an unsafe operation. The proposed scheme aims to establish the parameters of interest and/or patterns that may lead to unsafe wheelchair operations. This will further be implemented in an actual machine to maintain safe operations. Due to the sensitivity of the matter, a virtual environment is chosen for testing various environments. In this case, the study utilized an EOG-controlled wheelchair robot in a custom-made virtual environment designed in UNITY 3D platform. Using the customized data acquisition circuit, the system acquired horizontal eye movement at a sampling frequency of 192 Hz. Different classification algorithms were tested, and SVM was selected. Real-time control of the robotic wheelchair using commands from the classifier was achieved. This work's main contributions include i) using EOG for wheelchair control in a test/virtual simulation environment. ii) Determination of safe control parameters for wheelchair use.

The rest of the paper is presented in the following order. Section II discusses the materials, methods, and test simulation environments used in the research. In section III, the results of the simulations in the test environments a represented. Discussion and comparison of the result are given in section IV. Finally, conclusions are drawn in section V.

II. MATERIAL AND METHOD

Fig. 1 shows the different stages involved in the EOG control system. The EOG signal was acquired from horizontal eye movements and then passed through an analog/digital converter (ADC) which converted the analog signal voltages to digital values and passes it to MATLAB for processing. The signal was digitally filtered, and important and unique features were extracted to classify the eye movement as either right, left, or center.

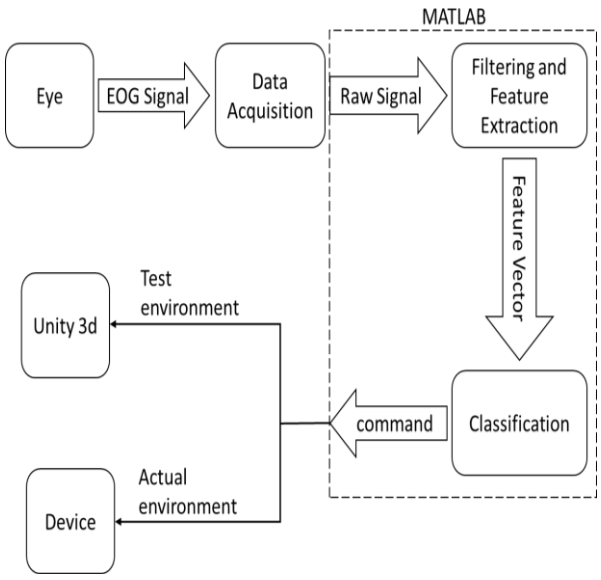

Fig. 1. Single channel Data Acquisition Circuit

A. EOG signal Acquisition and Processing

1) Acquisition

The EOG Data acquisition system was developed using filtering and amplification stages with a sampling frequency of 192 Hz and an overall gain of 95.55 dB, as in Fig. 3.

Three pre-gelled Ag/AgCl electrodes were used for the EOG signal acquisition, two on the outer canthus of each eye, and a third one that acted as a reference was placed on the forehead, as shown in Fig. 2.

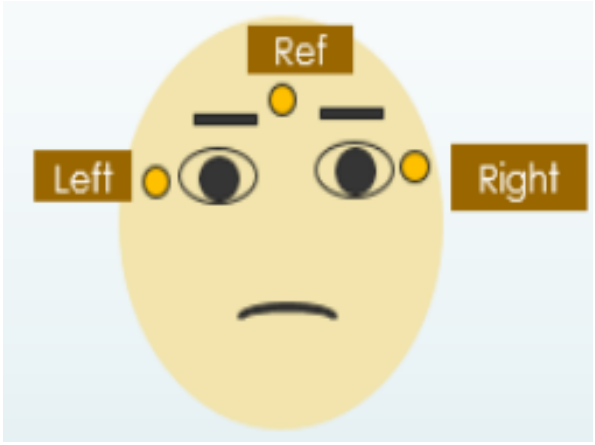

Fig. 2. Electrode Placement

The first stage of the circuit uses an instrumentation amplifier (AD620). The amplifier is chosen because of its ability to amplify the weak EOG signals from the electrodes while removing the common mode signal from the electrodes. AD620 was configured to a gain of 53.89dB using (1).

$$A = \frac{49.5k}{R4} + 1 \quad (1)$$

The signal from the instrumentation amplifier was fed into two cascaded non-inverting operational amplifiers (LM324) for more amplification of the EOG signals. The stages were cascaded to avoid amplifier saturation. The gain of each stage was set at 20.83 dB and is given by (2).

$$A = 1 + \frac{R7}{R6} = 1 + \frac{R10}{R9} \quad (2)$$

When collecting EOG signals, electromyogram (EMG) signals, power line noise, and intrinsic noise are primary noise sources. To eliminate the noise, an active band pass filter with a lower cut-off frequency of 0.02Hz and an upper cut-off frequency of 30Hz was used. The operational amplifier used was LM324 with a gain of 1 with a cut-off frequency calculated as shown in (3).

$$f_c = \frac{1}{2\pi RC} \quad (3)$$

For the lower cut-off stage: $R = R11$, $C = C3$, and for the upper cut-off stage: $R = R12$ and $C = C4$.

2) Digital Filtering

Signal processing of the collected EOG signal was done in MATLAB software. Single channel data acquisition circuit show in Fig. 3. Elimination of DC offset was done by subtracting the mean of the signal from the original signal.

Digital filtering was done using a Moving average filter (MAF) with a window length of 15 samples, as in Fig. 4. The filter reduces white noise to optimal levels and retains the sharp steep response, as shown in Fig. 4. The filter response is given by (4).

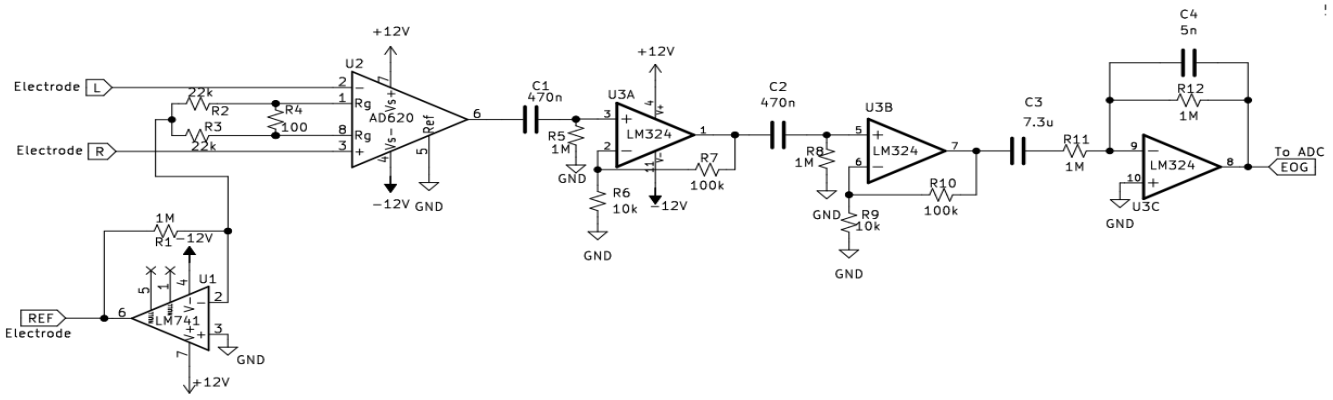

Fig. 3. Single channel Data Acquisition Circuit

$$y(n) = \ 1/M \sum\_(i = 0)\^(M - 1)\text{▒} \ 〚x[n + i]〛 \quad (4)$$

Where, M, n, x, *and* y represent the window size, the current sampling point, the raw signal, and the processed signal, respectively.

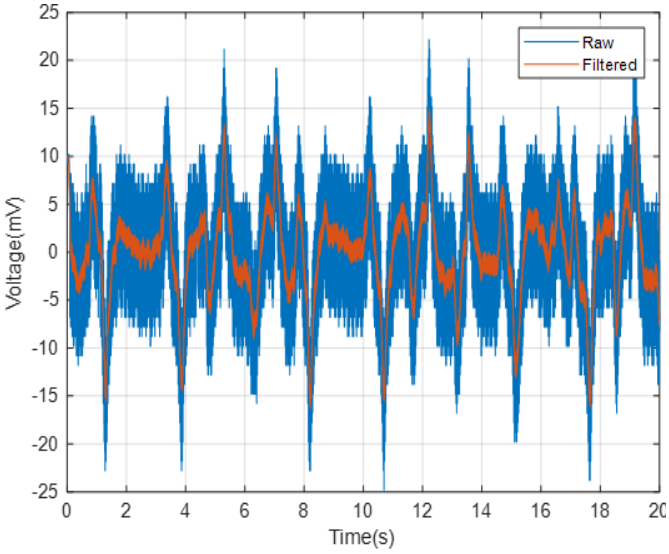

Fig. 4. Raw and filtered EOG signals using MAF.

The window length was settled upon after performing a Fast Fourier Transform (FFT) on the filtered signal with window lengths of 5, 10, and 15. The output of the FFT is shown in Fig 5. The window length of 15 filtered out high-frequency signal components while maintaining the envelope containing the gaze, which was essential to the work. Minimal change in the amplitude of the filtered signal compared to the raw signal is notable. However, this did not affect each gaze segment's critical and distinct characteristics.

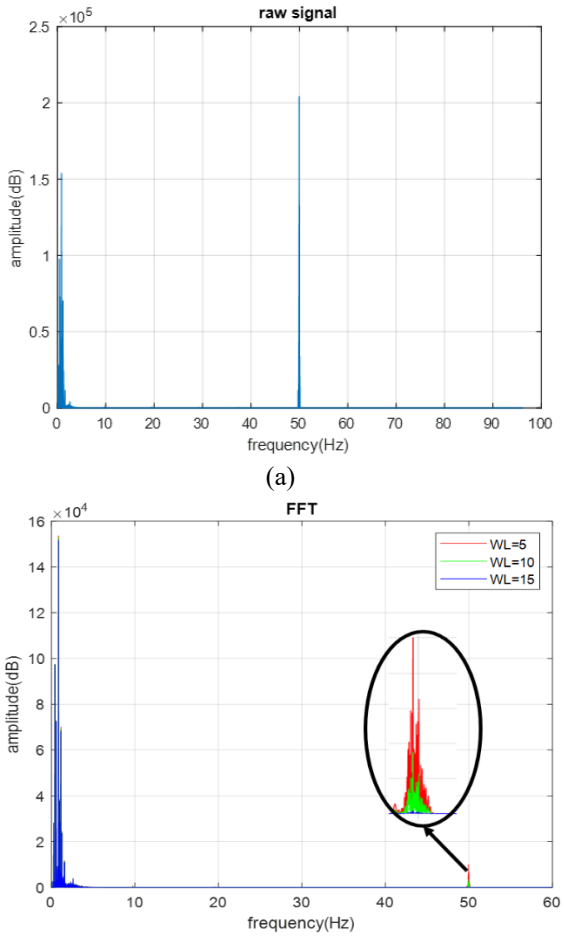

Fig. 5. Comparison of FFT output for different MAF window lengths: (a) FFT of the raw signal, (b) FFT of signal filtered with MAF of window lengths 5,10 and 15

B. *Machine learning and processing*

1) *Feature Extraction*

MATLAB software was used to extract different features from the processed signal for each segment of eye activity, i.e., left, right, and center. The extracted features were mean, variance, standard deviation, RMS, mean absolute deviation, mean frequency, and interquartile range. The entire signal

was segmented into 0.78 s long sections—each section representing left, right, or center. The length of the segment was determined by the timing of the control sequence when one looked either to the right or left and back to the center. Seven features were extracted for each section. This process assists in deriving patterns unique to the dataset without the risk of losing any essential information.

2) Classification

Classification is a process done on the extracted feature vectors to categorize patterns. Three classes were used for categorization; 0 for the center, 1 for the right, and −1 for the left. For training, the features extracted with their class labels from five subjects were combined and used for classification. The data were randomly divided into two portions, where 80% of the data was used for training while the other 20% was used for classifier prediction testing. Using the Classifier Learner Application (APP) toolbox in MATLAB, the five-fold cross-validation, the default setting for the APP, was used to initialize the hyper-parameter for the classifiers. Three classifiers that are the SVM, KNN, and Ensemble Bagged Tree, had the best performance in terms of accuracy and prediction time, as shown in Fig. 6. The confusion matrix in Fig. 7 shows the accuracy of the prediction of the classifiers for the individual classes and the misclassification rate of the same. The Support Vector Machine (SVM) classifier was identified as having the best performance with the highest accuracy and prediction time.

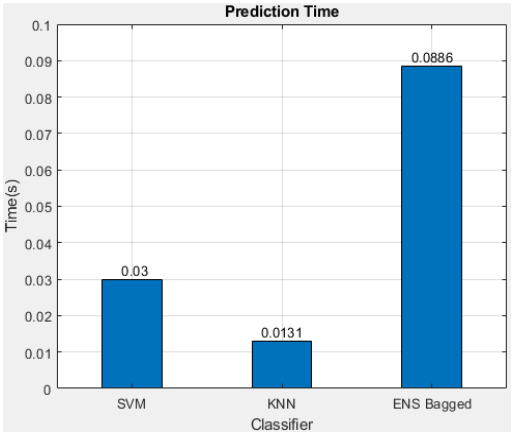

(a)

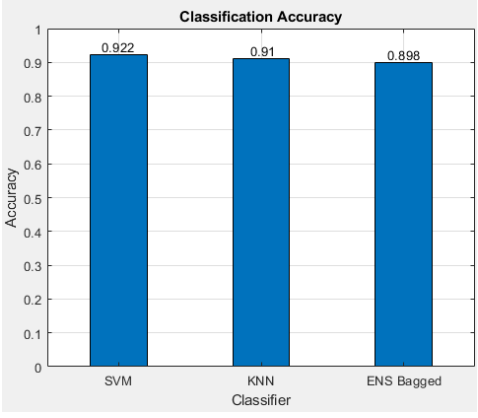

(b)

Fig. 6. Comparison of the performance of SVM, KNN, and Ensemble Bagged Tree classifiers: (a) accuracy and (b) prediction time

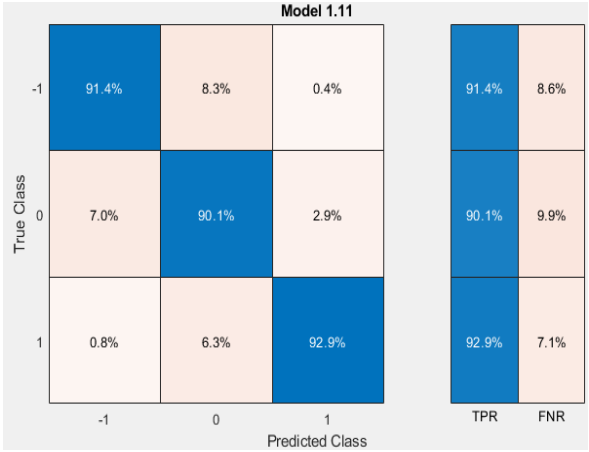

(a) SVM

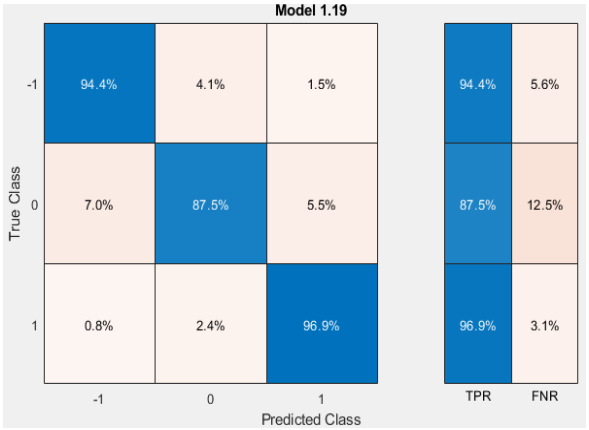

(b) KNN

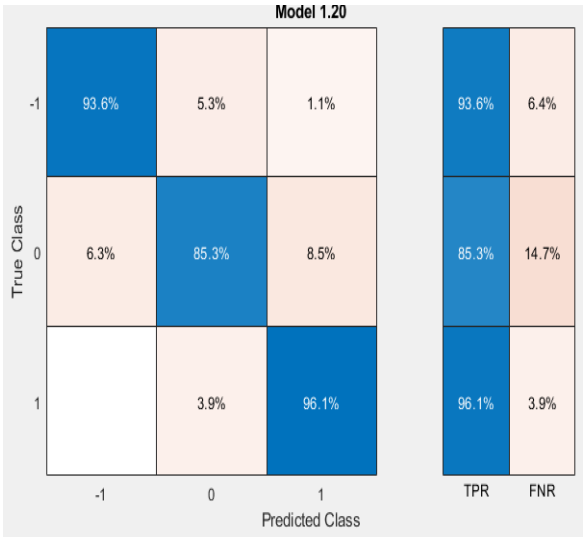

(c) Ensemble Bagged Tree

Fig. 7. Confusion matrix of SVM, KNN, and Ensemble bagged classifiers

3) Description of Control Signal

The control signal was generated by displaying a moving dot on a laptop screen approximately 1 meter away from the subject, as demonstrated in Fig. 8. The dot was centered on the screen at the onset of the recording but moved to either left or right randomly and back to the center after that. The direction of eye movement by the participants was as per the direction in which the dot appeared; otherwise, they maintained their eye position at the center until the dot moved. This was used as the control system for the

acquisition process that coincided with the EOG signal. A plot of a section of the recorded data and the control signal obtained is shown in Fig. 9.

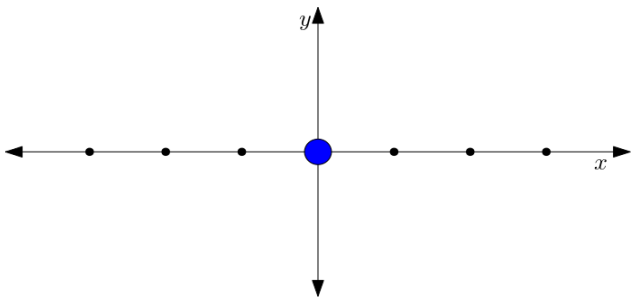

Fig. 8. Control layout

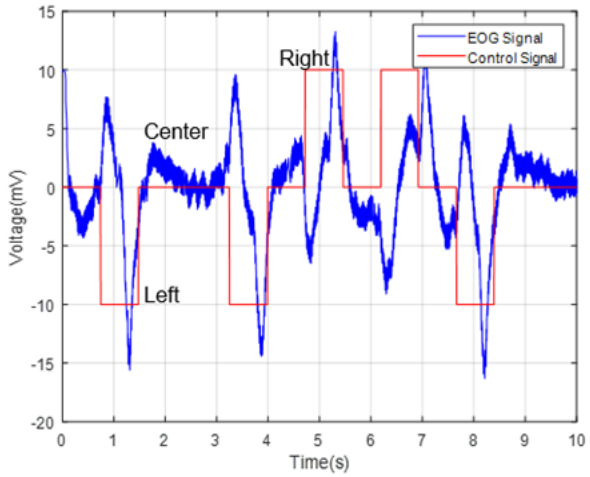

Fig. 9. EOG Signal and control signal

C. Control in Unity 3D

This paper used the Unity 3D game engine to develop the control scene. The built-in physics system of Unity 3D enabled us to confirm the collision/interaction of the robotic wheelchair with either the walls or the target object. In this case, the differential robot was controlled in the forward, left, or right directions using the commands generated in real-time by the SVM classifier in MATLAB. Unity 3D and MATLAB were connected through TCP/IP using a local host.

1) Differential Robot

The wheelchair model used in Unity 3D is a differential robot, as in the model in Fig. 10. The front wheel, a caster, is used for robot balancing, while the two rear wheels are used for driving the robot. The robot's direction can be changed by varying each rear wheel's relative rotation rate. The model works with the assumption that no wheels are slipping. When the wheels have the same speed, the robot moves straight while it moves either to the left or right, depending on the speed of both rear wheels [63]. The rear wheels' speeds vary by adjusting the voltage to each wheel through the different commands given.

The motion of the electric wheelchair, in a straight and rotating direction, is obtained as in (5) and (6);

$$v = \frac{r(\omega_R + \omega_L)}{2} \quad (5)$$

$$\psi = \frac{r(\omega_R - \omega_L)}{W} \quad (6)$$

The geometric and dynamic parameters are Velocity of the straight (yaw) motion (v, ψ), Radius of the rear wheels (r), Length of the wheelchair (L), Width of the wheelchair (W), Angular velocity of the left (right) wheel $(\omega L, \omega R)$, the centre of rotation (COR) and position in world coordinate system (x, y) [62].

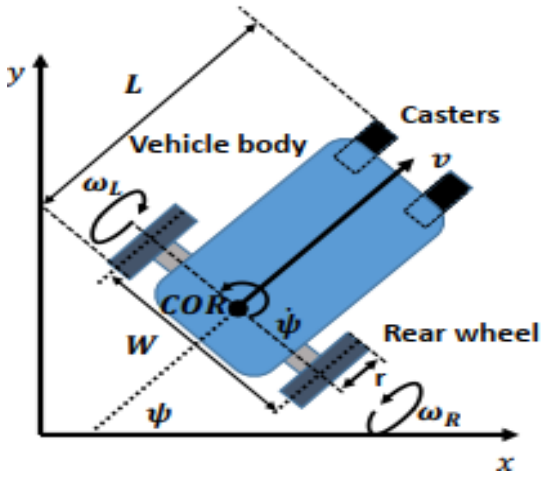

Fig. 10. Differential robot model of electric wheelchair [63]

2) Control Algorithm

Fig. 11 shows the flowchart for the control algorithm that describes how the command passed to Unity influences the direction of motion of the robot wheelchair. After processing the acquired EOG signal in MATLAB, the command is passed to Unity 3D software. If it is a 0 command, the left and right motors' speed remains unchanged, and the robot wheelchair keeps moving forward. However, when the command received is a 1, the speed (rpm) of the right motor is reduced for a specified time, making the robot turn in the right direction. When the command received is a -1, the speed (rpm) of the left motor is reduced for a specified time, making the robot turn in the left direction.

3) Control environments of interest

The driving experiments examined in this study are two: first, the forward movement of the robot and the minimum distance from the wall, and second turning around a corner as in Fig. 12.

While controlling an electric wheelchair, patients with a severe disability like tetraplegia are faced with two significant issues, collision with walls or obstacles and oversteering, as illustrated in Fig. 13. For successful control, these issues have to be minimized as much as possible. The environment and the problems faced by the patients are used to verify the work done in this study.

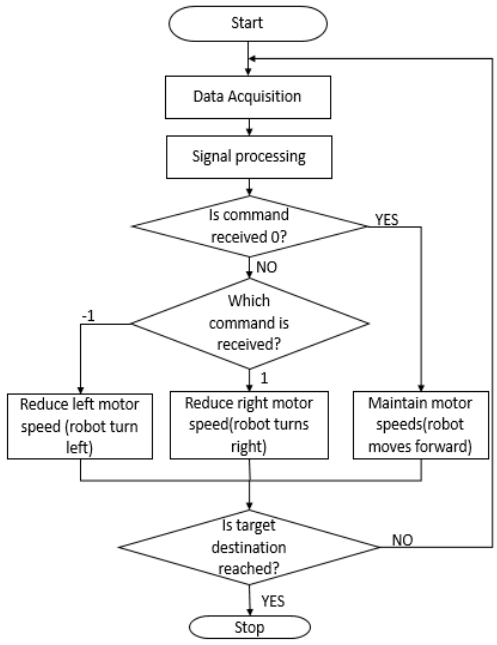

Fig. 11. Flowchart of the control algorithm.

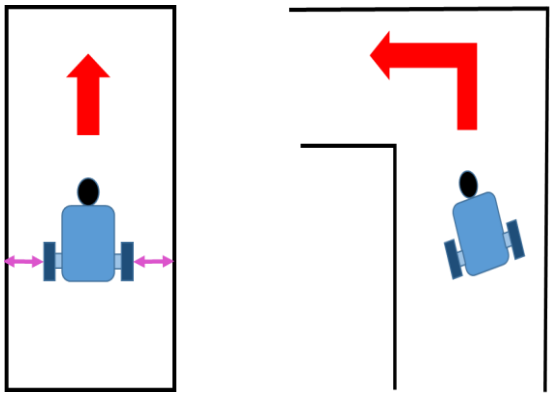

Fig. 12. Environments of control: (a) Forward motion and minimum distance from the wall and (b) Navigating a corner

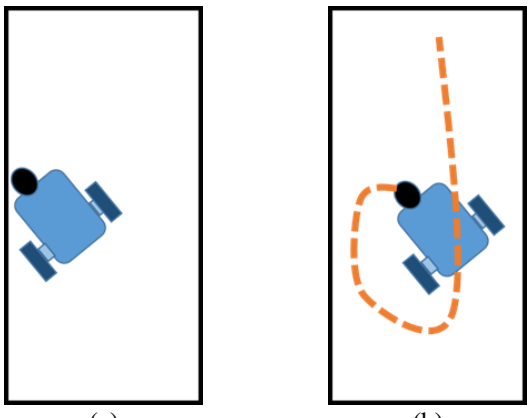

Fig. 13. Issues faced by disabled patients: (a) Collision and (b) Oversteering

4) Experiment 1: standard control test

The setup of the game mechanism is shown in Fig. 11(a). The experiment is set up with the maze divided into equal portions. The subject should control the differential robot from a predefined start point until a predefined endpoint. The subject can only move the robot in the forward, left, and right directions. Initially, the robot is in the bottom left corner of the maze and is set to move forward at a constant speed. Command 0 would keep the robot moving forward, and 1 and −1 would turn it to the right and left, respectively. Whenever the subject collides with a wall, the experiment is automatically started again until the robot is controlled to the target, which shows the game's success. The time taken for completion of the game and the trajectory length was recorded and used for analysis. In this experiment, the ability of different subjects to control the robotic wheelchair from the start to the target is tested.

5) Experiment 2: limit control test

The second experiment involved a modified scene, as in Fig. 11(b). The subjects are required to control the robotic wheelchair as they navigate the different sections until they get to the target. The experiment is designed so that sections (Sections 1-Section4) reduce in size as one navigates from the start to the target. Likewise, the gates (gate1-gate3) leading to the different sections also reduce in size. This experiment investigates the ability of the subjects to control the robot wheelchair in both large and small areas. Also, the navigation ability and the distances from the walls are considered. The robot's distance from nearby walls, sides, and front was recorded during control and used for analysis. Unity 3D layout shown in Fig. 14.

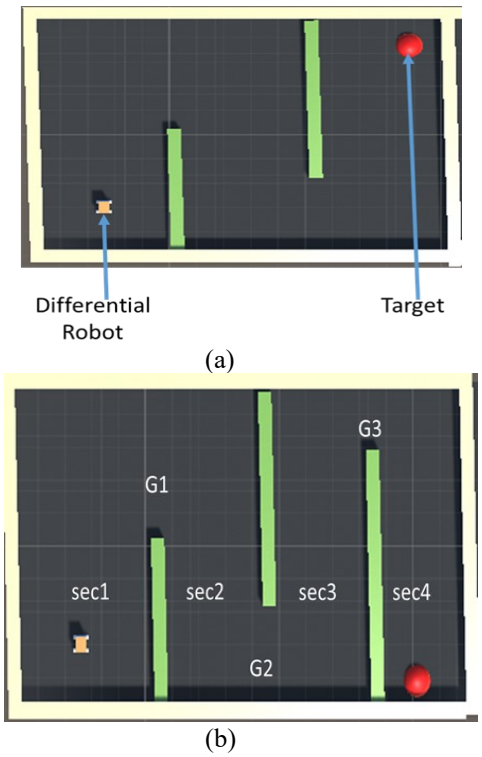

Fig. 14. Unity 3D layout: (a) Experiment one; (b) Experiment two (section as sec, gate as G)

D. Participants

A total of 22 healthy participants between the ages of 23-28 years took part in this experiment and were randomly selected (12 females, ten males). Six subjects were randomly selected among them to participate in data collection, while the rest participated in the control part of the study. Five subjects participated in experiment one, while eleven

participated in experiment two. None of the subjects who participated in the control had pre-exposure to the game scene. All participants provided their written consent following the approval procedures issued by the ethics committee of the Dedan Kimathi University of Technology University.

III. RESULT

Using the DAQ in Fig. 2, the horizontal EOG signal was acquired. A plot of horizontal eye signals is presented in Fig. 15. The EOG signal acquired had a frequency of 0.5 - 10Hz

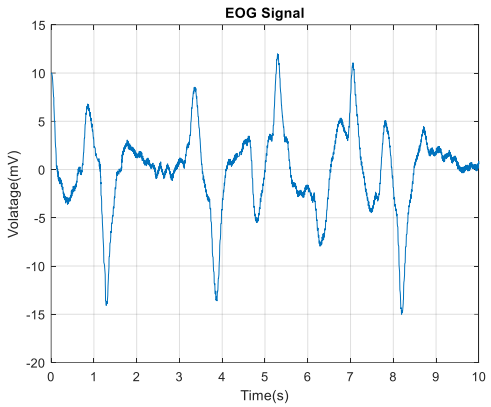

Fig. 15. Horizontal EOG Signal

When a subject moved his eyes from the center to the right and back to the center, the EOG signal had an initial negative peak accompanied by a positive, as indicated in Fig. 15. The amplitude of the negative peak is lower than that of the positive peak. This was caused by the cornea approaching the electrodes relative to the left eye's inner or outer canthus. When the subject looked to the left and back to the center, the behavior of the signal was inverted compared to the behavior of the right signal.

Only involuntary blinks are realized when the subject performs no activity (center); thus, the signal is not entirely flat or smooth during that time. These involuntary blinks, however, have insignificant amplitudes compared to the amplitude of right or left eye movement; hence, they cannot affect the control of the wheelchair. Furthermore, during classification, they were classified as a center.

A. Experiment 1

Real-time prediction of the eye signals was done for each of the five individuals selected for the system validation using the SVM classifier. The exact moving dot mechanism for data collection was used to direct individuals' eye movement. The performance indicators adopted for the evaluation of the system were from other studies [11], [40] and include:

1. Accuracy (A): Accuracy is the ratio of correct commands predicted (Nr) to the total commands issued (Nt) expressed as a percentage

$$\mathrm{A}(\%) = \frac{\mathrm{Nr}}{\mathrm{Nt}} \times 100 \tag{7}$$

2. Response time (RT): the total time taken in MATLAB to process a signal and generate a command

3. Information Transfer Rate (ITR): This measures the amount of information transferred in bits per minute. It is calculated as follows;

$$\mathrm{ITR\ (bits/min)} = \frac{60}{\mathrm{Tr}}\left[\mathrm{A}\log_2(\mathrm{A}) + (1-\mathrm{A})\log_2\left(\frac{1-\mathrm{A}}{\mathrm{Nt}-1}\right) + \log_2 \mathrm{Nt}\right] \tag{8}$$

where A is the average accuracy, Tr is the average response time, and Nt is the total number of commands.

The subjects participating in this experiment had no pre-exposure to the experiment. They experienced limited to no difficulty during the real-time control. All subjects showed high accuracy during the validation and good control of the robotic wheelchair, as presented in Table I. The system has an average accuracy of 96.54%, an RT of 0.7s, and an ITR of 579.60 bits/min. The high accuracy, ITR, and low response time are suitable for the system as it indicates how efficiently the system can be used in real-time as intended with fewer delays for command execution.

TABLE I. SYSTEM PERFORMANCE INDICES

Subject	A (%)	RT (s)	ITR (bits/min)
S1	100	0.7	/
S2	92.9	0.7	/
S3	97	0.7	/
S4	94.5	0.7	/
S5	99	0.7	/
Average	96.54	0.7	70.60

The performance of an individual in Unity 3D requires the subject to concentrate on the scene to make a turn and avoid a collision with the walls. The performance of the fastest and slowest subjects is displayed in Fig. 14. Both S1 and S2 managed to reach the target without any collision with the wall. However, Subject 2 experienced two instances of oversteering, which led The trajectory of the fastest subject (S1) and the slowest subject (S2) command inputs with the corresponding completion time shown in Fig. 16.

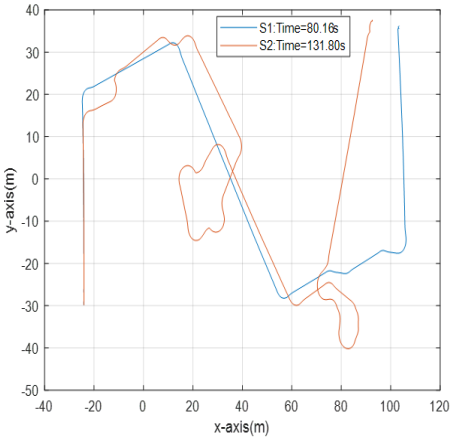

Fig. 16. The trajectory of the fastest subject (S1) and the slowest subject (S2) command inputs with the corresponding completion time

It is noted from Table II that subjects who took a shorter time to reach the target covered a shorter distance. The trajectory length was calculated as the sum of the x-y axis distances covered from the start point to the target. Longer

task time is associated with oversteering or wrong issuance of the input command. In this study, the fastest subject took 80.16s while the slowest subject took 131.80s. All five subjects in experiment 1 managed to control the robotic wheelchair to the target since the sections and gate regions were large. However, the time difference is noted due to the difference in the number of input commands issued.

TABLE II. SUBJECT PERFORMANCE

Subject	Task Time (s)	Trajectory Length(m)
S1	80.16	268.15
S2	131.80	378.87
S3	88.72	294.30
S4	86.98	290.36
S5	82.60	277.06

B. *Experiment two*

The system's performance was verified by eleven more subjects who participated in experiment 2. Using the shortest possible time, subjects were expected to control the robotic wheelchair through different sections to the target. The median is indicated by the red mark, while the top edge of the boxplot indicates the 75th percentile, and the bottom edge indicates the 25th percentile of a dataset. Red and blue '+' or 'o' signs indicates outliers in both cases. One of the parameters of concern while considering the safety of a wheelchair user is the distance from the wall as they control the robot on either a freeway or navigating a corner.

Since the sections and gates reduced in size as one approached the target, the minimum distances from the wall decreased, as in Fig. 17(a). The male subjects controlled the robot wheelchair much closer to the wall than their female counterparts, as shown in Fig. 17(b). Larger minimum distances from the wall guarantee the safety of the wheelchair user. The minimum distance from the wall at the gates also decreased as one approached the target, as indicated in Fig. 18(a) above. The male subjects achieved a larger minimum distance than the female subjects, as shown in Fig. 18(b).

In the sections, the female subjects performed better by achieving larger minimum distances from the wall than their male partners. On the contrary, the male subjects achieved larger minimum distances from the wall at the gates than the female. However, in both cases, the minimum distance interquartile range (IQR) for female subjects indicates more dispersion than the IQR for male subjects, as indicated in Table III.

This may suggest that the male subjects were more consistent in maintaining the distance from the wall than their female counterparts.

TABLE III. MINIMUM DISTANCE FROM THE WALL

Operation region	IQR		Mean ± SD
	Male	Female	
S1	4.063	7.983	9.85m ± 4.3
S2	0.342	8.5887	2.11m ± 3.51
S3	0.069	1.306	0.51m ± 1.51
S4	0.149	0.105	0.13m ± 0.08
G1	5.323	10.96	15.82m ± 7.93
G2	3.42	4.91	15.11m ± 3.48
G3	2.732	4.179	6.14m ± 2.69

NB: G is Gate, S is section

A comparison of the proposed system's performance to the state of art is made in Table IV. The evaluation is based on the accuracy, Response Time, Information Transfer Rate and the channels used in acquiring the signal. These parameters are important in evaluating a system as they depict the system's efficiency. A system should have a high prediction accuracy and low response time with a high ITR. Further, the systems considered used single-channel EOG signals, most of which were used for wheelchair control. The comparison indicates that the proposed system have comparatively better performance. A comparison of gender performance is shown in Fig. 19. The male subjects performed relatively better than the female subjects.

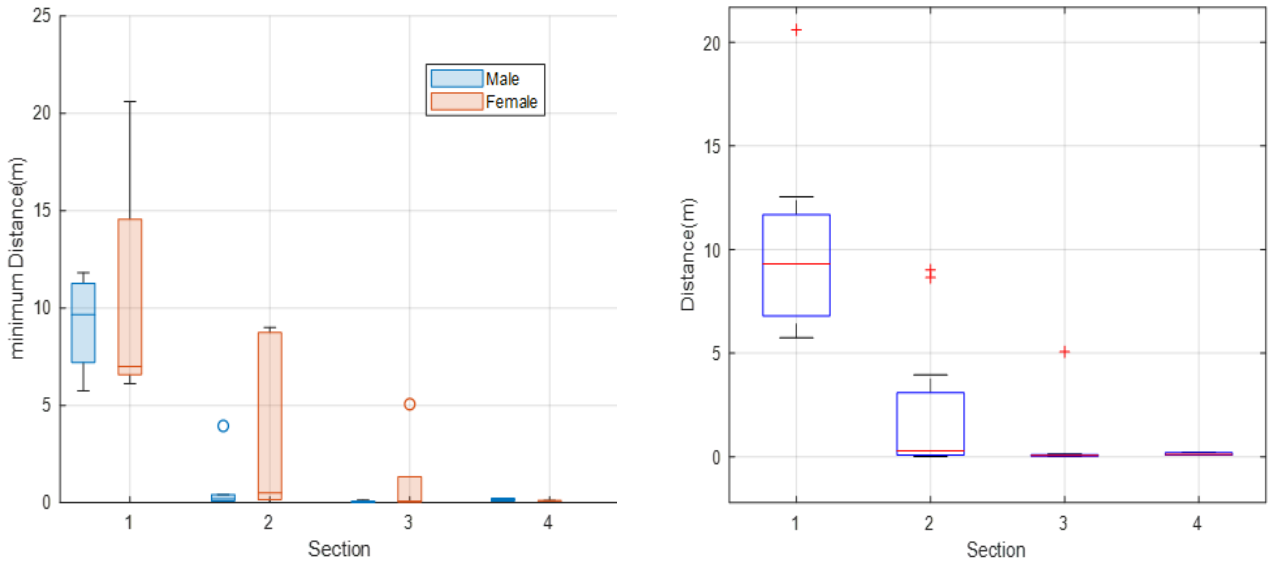

Fig. 17. Minimum distance from the wall: (a) (left) gender performance per section, (b) (right) all sections

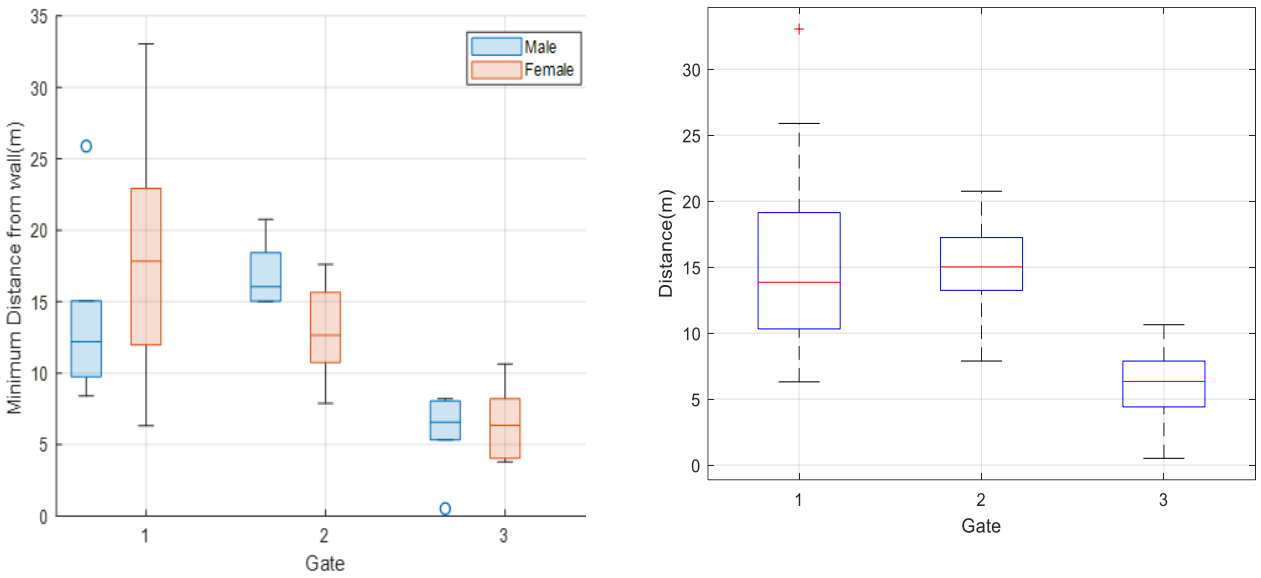

Fig. 18. Minimum distance from the wall: (a) gender performance per section, (b) all gates

TABLE IV. PERFORMANCE COMPARISON OF THE PROPOSED SYSTEM WITH STATE OF ART SYSTEMS

Author	Purpose	Signal	# channels	Accuracy (%)	RT(S)	ITR (bits/min)
He and Li [64]	Speller	EOG	1	94.13	4.14	68.69
Djeha *et al.* [60]	Wheelchair	EOG+ EEG	1	93	DNR	DNR
Kumar and Sharma [65]	Game control	EOG	2	78	DNR	DNR
Choudhari *et al.* [14]	Wheelchair	EOG	1	93.89	DNR	62.64
Li *et al* [26]	Wheelchair	EOG	1	99.5	1.3	DNR
Proposed approach	**Wheelchair**	**EOG**	**1**	**96.5**	**0.7**	**70.60**

Note: DNR denotes "did not report"

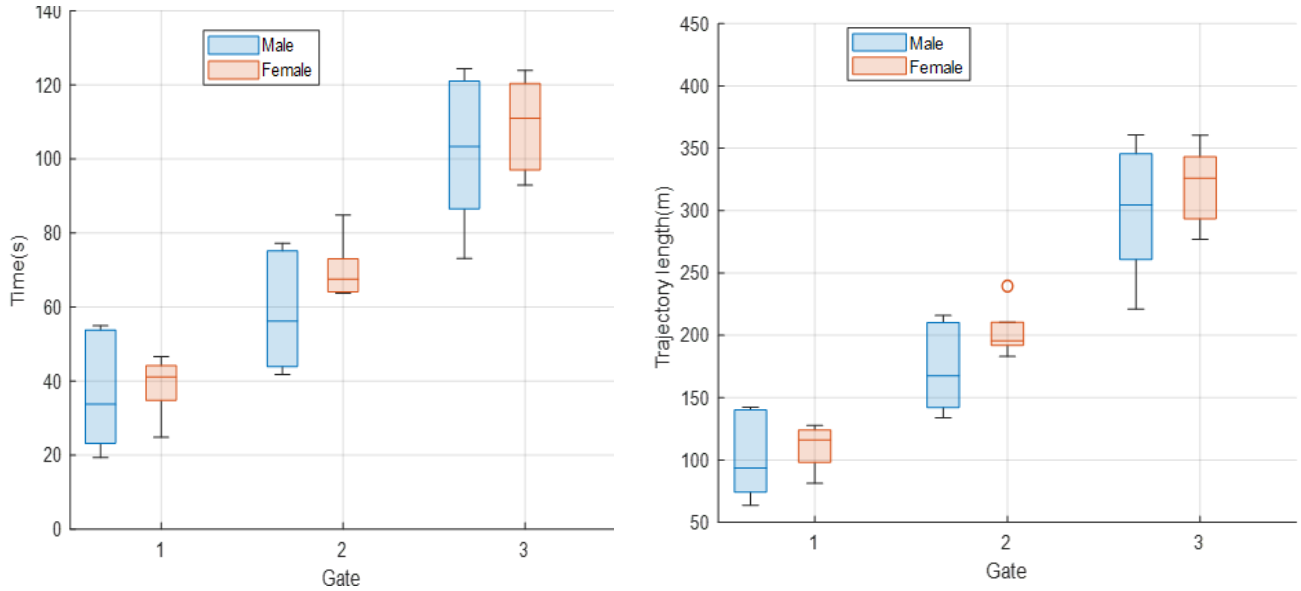

Fig. 19. Task Time and trajectory length to each gate for the male and female subjects

The male subjects took an average task time of 101.94s ±19.71 and a trajectory length of 287.31m ± 52.08, while the female took an average task time of 109.07s ± 13.25 and a trajectory length of 319.98m ± 32.68. This performance of the male subjects could be associated with their aggressiveness, while for females could be related to anxiety during control

Fig. 20 shows the trajectory of Subject 2, who took the shortest time to navigate to gate 3 and the goal, while subject 10 took the longest time and had instances of oversteering and a collision at gate 3. In the case of subject 10, the first instance of oversteering was on a reasonably larger area than the second. In the second instance, the subject almost hit the wall as the robot was closer to the wall. The work reported by authors in [60] indicates a successful control of a wheelchair in a virtual environment. In addition to analyzing the

successful control of the robot wheelchair, this study investigates the collision, oversteering, and safe control parameters of the electric wheelchair.

Depending on the trajectory taken by each subject, the time taken to gate 3 varies, as indicated in Table V. Subjects 1, 2, and 3 managed to control the robotic wheelchair to the target. Subjects 4, 5, 6, and 8 managed to control the wheelchair past gate 3 but hit the walls in section 4, while subjects 7, 9, 10, and 11 got to gate 3 and hit the walls at gate 3. Most subjects could not reach the target due to the challenges experienced during controlling the robotic wheelchair, like misclassification or unintentional issuance of wrong commands. These led to the subjects either colliding with the walls or having oversteering problems.

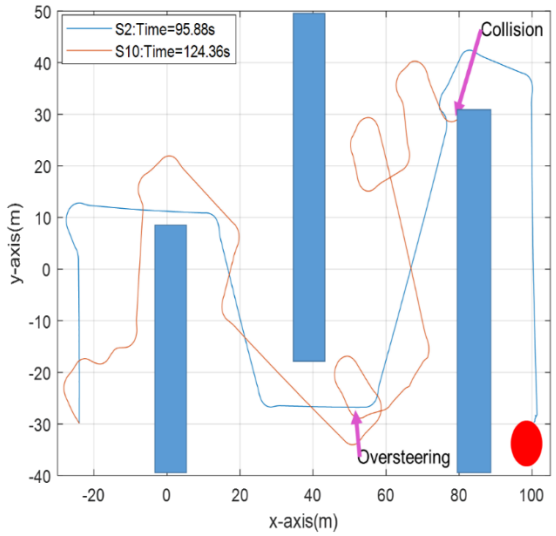

Fig. 20. The trajectory of the fastest subject (S2) and the slowest subject (S10) command inputs with the corresponding completion time and issues encountered

A few subjects managed to control the robot to the target, while six and eight subjects experienced oversteering and collision issues, respectively. Collisions were experienced in smaller sections while oversteering was experienced mainly in larger sections. In some instances, oversteering led to collisions with the wall, while in other cases, a subject managed to get back on track and control the robot to the destination.

TABLE V. PERFORMANCE OF SUBJECTS INDICATED BY TASK TIME AND CHALLENGES ENCOUNTERED

Subject	Time(s) to Gate3	Goal	Oversteering	Collision
1	86.48	✓	✓	×
2	73.12	✓	×	×
3	119.24	✓	×	×
4	98.36	×	×	✓
5	110.96	×	×	✓
6	102.26	×	✓	✓
7	123.88	×	×	✓
8	104.44	×	✓	✓
9	92.92	×	✓	✓
10	124.36	×	✓	✓
11	121	×	✓	✓

II. DISCUSSION

In this study, a robotic wheelchair is controlled in Unity 3D using horizontal saccadic eye movement. These eye movements control the wheelchair in the forward, right, and left directions. Two experiments were formulated to test the ability of different subjects to control the robot wheelchair.

From experiment 1, the system has an average accuracy of 96.54%, an RT of 0.7s, and an ITR of 70.60 bits/min. The high accuracy, ITR, and low response time are suitable for the system as it indicates how efficiently the system can be used in real-time as intended with fewer delays for command execution. From Table IV, the accuracy of this work of 96.54% is comparable to the accuracy of the study by Djeha *et al.* and Nam et al., which reported a value of 93% and 92.6% while using only single channel eye movement, respectively [60], [66]. The study by Kumar and Sharma in virtual reality game control using blinks and gaze reported a horizontal gaze accuracy of 80%.

The response time, which is the time the system takes to generate a command, should be as minimum as possible to ensure the shortest time delay between issuing and execution of the command. Compared to the 3.53s reported in [14] and 1.3s reported in [26], the response time of 0.7s obtained in this paper is better. The response time also significantly affects the ITR. ITR identifies the quantity of information a system's output can transmit. A high ITR achieved in this study of 70.6 bits/min guarantees faster communication between MATLAB and Unity without losing information as desired. Further, the performance of the proposed system is attributed to the classifier used and the signal processing method. The ability of the system to generalize makes it better than the others since no recalibration is needed when new individuals are using it.

All five subjects in experiment 1 managed to control the robotic wheelchair to the target since the sections and gate regions were large. The trained model generalized satisfactorily across all participants without requiring recalibration or retraining, which enhanced the usability and simplicity of the setup. However, the time difference is noted due to the difference in the number of input commands issued.

In experiment 2, a test was done to determine the safe control parameter by recording the limit or minimum distance from the wall for both the sections and the gate regions of the experiment environment. Subjects, if possible, are to maintain the position of the robotic wheelchair at the center of the sections and the gate area. In section 1, the average minimum distance achieved was 9.85m ± 4.3, while in sections 2, 3, and 4, the average minimum distance was 2.11m ± 3.51, 0.51m ± 1.51, and 0.13m ± 0.08, respectively. At the gates, the average minimum distance achieved was 15.82m ± 7.93, 15.11m ± 3.48, and 6.14m ± 2.69 for gates 1, 2, and 3, respectively, as presented in Table III. From this it can be inferred that the safety of the wheelchair is mostly affected in sections with smaller operating regions as the distances between the wheelchair and the wall in this section is very small.

By monitoring the distances, the user's safety can be ensured during control, especially when misclassification occurs or when a wrong command is issued. When these occur, the user's safety is jeopardized, especially when the wheelchair is near an obstacle. This is because a false command would steer the wheelchair in an undesired direction which may be risky for the user and those around them.

Both genders experienced collisions and oversteering during control in the second scene, where 72% and 54% instances of collision and oversteering were reported, respectively. Notably, the collisions occurred in small-sized sections. From this, it is critical to consider the complexity of the control environment and the sufficiency of the control skills of the participants to ensure safety in operations.

By exposing wheelchair users to different environments with different complexities in the virtual environment setup, the user's gain more skill of navigation and control. These skills can be transferred for use in real-world environment as reported in [59]. Further, with the developed environments, the wheelchair users can training more and repeatedly until they are confident then they can use actual wheelchair. Authors in [62] noted that the steering ability of individuals could be improved when subjects are allowed multiple trial runs to familiarize themselves with the control environment. This helps in improving the safety of the user and those around them.

From the research finding, one of the safety parameters that should be considered is the distances from the walls and/or obstacles. User safety can be jeopardized in instance of a misclassification and/or unintentional command issued. These challenges are out of control of the user and are the major causes of collision and oversteering. In a practical case, incorporating the safe distance auto-piloting mechanism used for auto control can be essential to monitor the minimum distance from the wall, thus protecting the patients from a collision.

The strength of this study is the ability of individuals to control the robot wheelchair in different environments successfully without the need for recalibration or retraining since the trained model generalized satisfactorily across all participants which enhanced the usability and simplicity of the setup.

One of the drawbacks of this study is that persons with disabilities (PWD), sick individuals, or any ALS individuals who are the intended users of the device were not included as subjects. Thus we were not able to analyze the control issues with this group. The performance achieved with healthy subjects is essential in fine-tuning control algorithms. This work has not yet been implemented in an actual environment that involves the intended group of individuals.

III. CONCLUSION

This study has presented a novel horizontal EOG signal control of a robotic wheelchair designed in a Unity 3D virtual environment. Using three commands, the wheelchair was controlled in real-time, i.e., in the forward, left, and right directions. The system obtained an average classifier accuracy of 96.54%, with an RT of 0.7s and an ITR of 70.60 bits/min. As the operating sections reduce in size, the subjects are expected to have a higher concentration to maintain a safe distance from the wall. Different subjects take a different amount of time to control the robot to the desired location. This is due to the difference in the number of input commands issued. Cases of misclassification and issuing of unintentional commands may lead to collision and oversteering hence jeopardizing the wheelchair user's safety. It was determined that one of the safety parameters to be considered for wheelchair users is the distance from the walls, in freeways, and while navigating a corner. With the reported performance, the setup can be implemented in a physical setup with little fine-tuning in the algorithm to accommodate the target user. Since this study focuses on persons with severe disabilities, their safety is paramount; hence to facilitate better control in a physical environment, the speed of the wheelchair should be keenly considered.

In the future, the work can be implemented in a real-world environment, where the minimum distance from the wall would be recorded. Subsequent work may address this by expanding the work to a more representative sample and physical implementations. Also, the system can be hybridized by combining EOG with other bio-signals for control. To use this system in a real-world environment, it is recommended that potential users perform the tests presented in a virtual environment to familiarize themselves with the environment. Satisfactory results should be obtained before subjects are exposed to the real-world environment. Also, more research should be done to increase the number of control commands while avoiding overcomplicating the system.

ACKNOWLEDGMENT

This work was supported by the Kenya Education Network (KENET) award of the Research and Innovation Grant in Engineering 2022/2023.

REFERENCES

[1] M. Sasaki, M. Syaiful, A. Bin Suhaimi, K. Matsushita, S. Ito, and M. I. Rusydi, "Robot Control System Based on Electrooculography and Electromyogram," *J. Comput. Commun.*, vol. 03, no. 11, pp. 113–120, 2015.

[2] L. Wagner, "Disabled People in the World: Facts and Figures," 2021. [Online]. Available: https://www.inclusivecitymaker.com/disabled-people-in-the-world-in-2021-facts-and-figures/

[3] S. Heera and A. Maini, "Disability Inclusion," *Flexible Strategies in VUCA Markets2018*, pp. 79–88, 2018.

[4] M. Callejas-Cuervo, A. X. González-Cely, and T. Bastos-Filho, "Control Systems and Electronic Instrumentation Applied to Autonomy in Wheelchair Mobility: The State of the Art," *Sensors*, vol. 20, no. 21, p. 6326, 2020.

[5] Z. T. Al-qaysi, B. B. Zaidan, A. A. Zaidan, and M. S. Suzani, "A review of disability EEG based wheelchair control system: Coherent taxonomy, open challenges and recommendations," *Comput. Methods Programs Biomed.*, vol. 164, pp. 221–237, 2018.

[6] J. H. Choi, Y. Chung, and S. Oh, "Motion control of joystick interfaced electric wheelchair for improvement of safety and riding comfort," *Mechatronics*, vol. 59, pp. 104–114, 2019.

[7] M. Shibata, C. Zhang, T. Ishimatsu, M. Tanaka, and J. Palomino, "Improvement of a Joystick Controller for Electric Wheelchair User," *Mod. Mech. Eng.*, vol. 05, pp. 132–138, 2015.

[8] M. Mrabet, Y. Rabhi, and F. Fnaiech, "Development of a New Intelligent Joystick for People with Reduced Mobility," *Appl. bionics Biomech.*, vol. 2018, p. 2063628, 2018.

[9] L. Yang, N. Guo, R. Sakamoto, N. Kato, and K. Yano, "Electric

Wheelchair Hybrid Operating System Coordinated with Working Range of a Robotic Arm," *J. Robot. Control*, vol. 3, no. 5, pp. 679–689, 2022.

[10] S. Anwer *et al.*, "Eye and Voice-Controlled Human Machine Interface System for Wheelchairs Using Image Gradient Approach," *Sensors*, vol. 20, no. 19, 2020.

[11] V. Khare, S. Gupta, and K. Meena, "Voice Controlled Wheelchair," *Int. J. Electron. Electr. Comput. Syst.*, vol. 6, no. 4, 2017.

[12] R. Berjón, M. Mateos, A. Barriuso, I. Muriel, and G. Villarrubia, "Head Tracking System for Wheelchair Movement Control," in *Highlights in Practical Applications of Agents and Multiagent Systems*, pp. 307–315, 2011.

[13] S. Udhaya kumar and V. M. Vinod, "EOG based wheelchair control for quadriplegics," in *2015 International Conference on Innovations in Information, Embedded and Communication Systems (ICIIECS)*, pp. 1–4, 2015.

[14] A. M. Choudhari, P. Porwal, V. Jonnalagedda, and F. Mériaudeau, "An Electrooculography based Human Machine Interface for wheelchair control," *Biocybern. Biomed. Eng.*, vol. 39, no. 3, pp. 673–685, 2019.

[15] N. M. M. Noor and S. Ahmad, "Analysis of different EOG-based eye movement strength levels for wheelchair control," *Int. J. Biomed. Eng. Technol.*, vol. 11, no. 2, p. 175, 2013.

[16] W.-D. Chang, "Electrooculograms for Human-Computer Interaction: A Review," *Sensors*, vol. 19, no. 12, p. 2690, 2019.

[17] H. Wang, Y. Li, J. Long, T. Yu, and Z. Gu, "An asynchronous wheelchair control by hybrid EEG-EOG brain-computer interface," *Cogn. Neurodyn.*, vol. 8, no. 5, pp. 399–409, 2014.

[18] J. K. Muguro *et al.*, "Development of Surface EMG Game Control Interface for Persons with Upper Limb Functional Impairments," *Signals*, vol. 2, no. 4, pp. 834–851, 2021.

[19] U. Chaudhary, N. Birbaumer, and A. Ramos-Murguialday, "Brain–computer interfaces for communication and rehabilitation," *Nat. Rev. Neurol.*, vol. 12, no. 9, pp. 513–525, 2016.

[20] Q. Huang, Z. Zhang, T. Yu, S. He, and Y. Li, "An EEG-/EOG-Based Hybrid Brain-Computer Interface: Application on Controlling an Integrated Wheelchair Robotic Arm System," *Front. Neurosci.*, vol. 13, 2019.

[21] M. Sasaki *et al.*, "Robot control systems using bio-potential signals," in *THE 5TH International Conference on Industrial, Mechanical, Electrical, and Chemical Engineering2019 (ICIMECE 2019)*, 2020.

[22] M. Plugovoy, M. Forde, T. Wang, E. Chabot, and Y. Sun, "Integrated EOG and EMG Front-End for Differentiating Intentional and Unintentional Blinks," *43rd Annual Northeast Bioengineering Conference*, 2017.

[23] T. Triwiyanto, W. Caesarendra, V. Abdullayev, A. A. Ahmed, and H. Herianto, "Single Lead EMG signal to Control an Upper Limb Exoskeleton Using Embedded Machine Learning on Raspberry Pi," *J. Robot. Control*, vol. 4, no. 1, pp. 35–45, 2023.

[24] N. S. Shalal and W. Aboud, "Smart Robotic Exoskeleton: a 3-DOF for Wrist-forearm Rehabilitation," *J. Robot. Control*, vol. 2, no. 6, pp. 476--483, 2021.

[25] V. Ratne and M. S. Panse, "Single Channel EOG Signal Processing and Features Extraction using Virtual Instrumentation," in *International Journal of Research and Scientific Innovation (IJRSI)*, vol. 5, no. 4, 2018.

[26] Y. Li, S. He, Q. Huang, Z. Gu, and Z. L. Yu, "A EOG-based switch and its application for start/stop control of a wheelchair," *Neurocomputing*, vol. 275, pp. 1350–1357, 2018.

[27] M. R. Chowdhury, M. N. Mollah, M. Raihan, A. S. Ahmed, M. A. Halim, and M. S. Hossain, "Designing a Cost Effective Prototype of an Automated Wheelchair Based on EOG (Electrooculography)," in *2018 21st International Conference of Computer and Information Technology (ICCIT)*, 2018.

[28] M. Talukder, Rawdah, A. Aktar, A. Neelima, and A. Rahman, "EOG Based Home Automation System by Cursor Movement Using a Graphical User Interface (GUI)," in *2018 IEEE International WIE Conference on Electrical and Computer Engineering (WIECON-ECE)*, 2018.

[29] L. Subramanyan, G. Babu, S. Divya, S. Sampley, and S. Yuvaraj, "An approach to control appliances using EOG signal for physically challenged persons," *Int. J. Pure Appl. Math.*, vol. 119, pp. 285–295, 2018.

[30] D. R. Lingegowda, K. Amrutesh, and S. Ramanujam, "Electrooculography based assistive technology for ALS patients," in *2017 IEEE International Conference on Consumer Electronics-Asia (ICCE-Asia)*, pp. 36-40, 2017.

[31] A. Larson, J. Herrera, K. George, and A. Matthews, "Electrooculography based electronic communication device for individuals with ALS," in *2017 IEEE Sensors Applications Symposium (SAS)*, pp. 1-5, 2017.

[32] A. López, F. Ferrero, D. Yangüela, C. Álvarez, and O. Postolache, "Development of a Computer Writing System Based on EOG," *Sensors*, vol. 17, no. 7, p. 1505, 2017.

[33] P. Shanmugam, "A Novel Analysis of EOG Through Labview for Prosthetic Arm Control System Design Using PIC Microcontroller," *Int. J. Eng. Sci. Invent. Res. Dev.*, vol. 5, no. 8, 2019.

[34] S. S. Dhankar and M. Soni, "Development of an Eog Based Human Machine Interface to Control a 3R Robot," *Int. J. Adv. Res. Innov. Ideas Educ.*, vol. 2, pp. 237–243, 2016.

[35] M. Sivakumar, B. Abukalam, R. A. Kumar, S. A. Kumar, and M. H. R. Moorthy, "Microcontroller Based EOG Wheelchair," *Int. J. Innov. Res. Sci. Eng. Technol.*, vol. 8, pp. 49–52, 2019.

[36] R. B. Navarro, L. B. Vázquez, and E. L. Guillén, "EOG-based wheelchair control," in *Smart Wheelchairs and Brain-Computer Interfaces*, pp. 381–403, 2018.

[37] Z. Hossain, M. M. H. Shuvo, and P. Sarker, "Hardware and software implementation of real time electrooculogram (EOG) acquisition system to control computer cursor with eyeball movement," in *2017 4th International Conference on Advances in Electrical Engineering (ICAEE)*, pp. 132–137, 2017.

[38] D. B. Anagha, M. S. Sowmya, S. Bhavani, R. N. Priya, and M. R. Usha, "Eye Gaze Controlled Wheelchair," *Int. J. Eng. Res.*, vol. 9, no. 5, 2020.

[39] B. Champaty, J. Jose, K. Pal, and A. Thirugnanam, "Development of EOG based human machine interface control system for motorized wheelchair," in *2014 Annual International Conference on Emerging Research Areas: Magnetics, Machines and Drives (AICERA/iCMMD)*, pp. 1-7, 2014.

[40] N. Borkar, T. Dongare, P. Chahande, J. Bonsod, and A. B. Jirapure, "Microcontroller Based EOG and Accelerometer Guide Wheelchair," *Int. Res. J. Eng. Technol.*, vol. 5, no. 3, pp. 3803–3807, 2018.

[41] A. Rajesh and M. Mantur, "Eyeball gesture controlled automatic wheelchair using deep learning," in *2017 IEEE Region 10 Humanitarian Technology Conference (R10-HTC)*, pp. 387-391, 2017.

[42] Q. Huang *et al.*, "An EOG-Based Human-Machine Interface for Wheelchair Control," *{IEEE} Trans. Biomed. Eng.*, vol. 65, no. 9, pp. 2023–2032, 2018.

[43] A. Goil, M. Derry, and B. D. Argall, "Using machine learning to blend human and robot controls for assisted wheelchair navigation," in *2013 IEEE 13th International Conference on Rehabilitation Robotics (ICORR)*, p. 1-6, 2013.

[44] F. D. Pérez-Reynoso, L. Rodriguez-Guerrero, J. C. Salgado-Ramirez, and R. Ortega-Palacios, "HumanMachine Interface: Multiclass Classification by Machine Learning on 1D EOG Signals for the Control of an Omnidirectional Robot," *Sensors*, vol. 21, no. 17, p. 5882, 2021.

[45] A.-G. A. Abdel-Samei, A. S. Ali, F. E. A. El-Samie, and A. M.Brisha, "Efficient Classification of Horizontal And Vertical EOG Signals For Human Computer Interaction," *Research Square,* 2021.

[46] J. Martínez-Cerveró *et al.*, "Open Software/Hardware Platform for Human-Computer Interface Based on Electrooculography (EOG) Signal Classification," *Sensors*, vol. 20, no. 9, p. 2443, 2020.

[47] X. Wang, Y. Xiao, F. Deng, Y. Chen, and H. Zhang, "Eye-Movement-Controlled Wheelchair Based on Flexible Hydrogel Biosensor and WT-SVM," *Biosensors*, vol. 11, no. 6, p. 198, 2021.

[48] F. A. Azhar *et al.*, "The Classification of Electrooculogram (EOG) Through the Application of Linear Discriminant Analysis (LDA) of Selected Time-Domain Signals," in *Lecture Notes in Electrical Engineering*, pp. 583–591, 2021.

[49] Babita, P. Syal, and P. Kumari, "Comparative Analysis of KNN,

SVM, DT for EOG based Human Computer Interface," in *2017 International Conference on Current Trends in Computer, Electrical, Electronics and Communication (CTCEEC)*, pp. 1023–1028, 2017.

[50] F. A. Alturki, K. AlSharabi, A. M. Abdurraqeeb, and M. Aljalal, "EEG Signal Analysis for Diagnosing Neurological Disorders Using Discrete Wavelet Transform and Intelligent Techniques.," *Sensors (Basel).*, vol. 20, no. 9, 2020.

[51] Q. Zhang *et al.*, "A real-time wireless wearable electroencephalography system based on Support Vector Machine for encephalopathy daily monitoring," *Int. J. Distrib. Sens. Networks*, vol. 14, no. 5, p. 1550147718779562, 2018.

[52] A. Abdelsamei, A. Ali, F. Abd El-Samie, and A. Brisha, "Efficient Classification of Horizontal And Vertical EOG Signals For Human Computer Interaction," *Research Square*, 2021.

[53] T. hussein Onn, "Analysis of Electroculography (EOG) for Controlling Wheelchair Motion," *Doctoral dissertation, Universiti Tun Hussein Onn Malaysia*, 2015.

[54] L. J. Qi and N. Alias, "Comparison of ANN and SVM for classification of eye movements in EOG signals," *J. Phys. Conf. Ser.*, vol. 971, p. 12012, 2018.

[55] C. Genova *et al.*, "A simulator for both manual and powered wheelchairs in immersive virtual reality CAVE," *Virtual Real.*, vol. 26, no. 1, pp. 187–203, 2022.

[56] H. Younis, F. Ramzan, J. Khan, and M. U. Ghani Khan, "Wheelchair Training Virtual Environment for People with Physical and Cognitive Disabilities," in *2019 15th International Conference on Emerging Technologies (ICET)*, pp. 1–6, 2019.

[57] M. Eidel and A. Kübler, "Wheelchair Control in a Virtual Environment by Healthy Participants Using a P300-BCI Based on Tactile Stimulation: Training Effects and Usability," *Front. Hum. Neurosci.*, vol. 14, p. 265, 2020.

[58] L. Keeler, R. L. Kirby, K. Parker, K. D. McLean, and J. A. Hayden, "Effectiveness of the Wheelchair Skills Training Program: a systematic review and meta-analysis.," *Disabil. Rehabil. Assist. Technol.*, vol. 14, no. 4, pp. 391–409, 2019.

[59] C. Bigras, D. Kairy, and P. S. Archambault, "Augmented feedback for powered wheelchair training in a virtual environment," *J. Neuroeng. Rehabil.*, vol. 16, no. 1, p. 12, 2019.

[60] M. Djeha, F. Sbargoud, M. Guiatni, K. Fellah, and N. Ababou, "A combined EEG and EOG signals based wheelchair control in virtual environment," in *2017 5th International Conference on Electrical Engineering - Boumerdes (ICEE-B)*, pp. 1–6, 2017.

[61] A. P. S. Haroon and D. R. Premachand, "Human Activity Recognition using Machine Learning Approach," *J. Robot. Control*, vol. 2, no. 5, pp. 395–399, 2021.

[62] L. Xi and M. Shino, "Shared Control Design Methodologies of an Electric Wheelchair for Individuals with Severe Disabilities using Reinforcement Learning," *J. Adv. Simul. Sci. Eng.*, vol. 7, pp. 300–319, 2020.

[63] R. Socas, S. Dormido, and R. Dormido, "Optimal Threshold Setting for Event-Based Control Strategies," *IEEE Access*, vol. 5, p. 2880-2893, 2017.

[64] S. He and Y. Li, "A Single-Channel EOG-Based Speller," *IEEE Trans. Neural Syst. Rehabil. Eng.*, vol. 25, no. 11, pp. 1978–1987, 2017.

[65] D. Kumar and A. Sharma, "Electrooculogram-based virtual reality game control using blink detection and gaze calibration," in *2016 International Conference on Advances in Computing, Communications and Informatics (ICACCI)*, pp. 2358–2362, 2016.

[66] Y. Nam, B. Koo, A. Cichocki, and S. Choi, "GOM-Face: GKP, EOG, and EMG-Based Multimodal Interface With Application to Humanoid Robot Control," *IEEE Trans. Biomed. Eng.*, vol. 61, no. 2, pp. 453–462, 2014.